

Density Functional Studies of Coenzyme NADPH and Its Oxidized Form NADP⁺: Structures, UV–Vis Spectra, and the Oxidation Mechanism of NADPH

Xiaoyan Cao *,^[a] Liangliang Wu,^[a,b] Jun Zhang,^[c] and Michael Dolg*,^[a]

Density functional theory has been used to study the biologically important coenzyme NADPH and its oxidized form NADP⁺. It was found that free NADPH prefers a compact structure in gas phase and exists in more extended geometries in aqueous solution. Ultraviolet–visible absorption spectra in aqueous solution were calculated for NADPH with an explicit treatment of 100 surrounding water molecules in combination with the COSMO solvation model for bulk hydration effects. The obtained spectra using the B3LYP hybrid density functional agree quite well with experimental data. The changes of Gibbs free energies ΔG in reactions of NADPH with O₂ observed experimentally in cardiovascular and in chemical systems, that is, $\text{NADPH} + 2 \text{}^3\text{O}_2 \rightarrow \text{NADP}^+ + 2 \text{O}_2^- + \text{H}^+$ and NADPH

$+ \text{}^1\text{O}_2 + \text{H}^+ \rightarrow \text{NADP}^+ + \text{H}_2\text{O}_2$, respectively, were calculated. The NADPH oxidation reaction in the cardiovascular system cannot proceed without activation since the obtained ΔG is positive. The reaction of NADPH in the chemical system with singlet oxygen was found to proceed in two ways, each consisting of two steps, that is, NADPH firstly reacts with $\text{}^1\text{O}_2$ barrierlessly to form NADP⁺ and HO₂⁻, from which H₂O₂ is formed in a spontaneous reaction with H⁺, or $\text{}^1\text{O}_2$ and H⁺ initially form $\text{}^1\text{HO}_2^+$, which further reacts with NADPH to yield NADP⁺ and H₂O₂. © 2019 The Authors. *Journal of Computational Chemistry* published by Wiley Periodicals, Inc.

DOI: 10.1002/jcc.26103

Introduction

NAD(P)H (nicotinamide adenine dinucleotide (phosphate)) and its derivatives play an essential role as universal coenzymes in a large variety of biochemical processes in both plants and animals.^[1,2] The reduced form NAD(P)H can (formally) provide a hydride ion (H⁻) for chemical reactions to end up in the oxidized form NAD(P)⁺. NAD(P)H can thus be considered as a storage for a hydride ion, or the equivalent of two electrons and a proton as well as a related amount of energy. A large variety of enzymes uses NAD(P)H, for example, reductases, oxygenases and dehydrogenases. In a simple model the reduced/oxidized coenzyme forms a temporary complex with the enzyme, enabling a specific chemical reaction, after which the then oxidized/reduced coenzyme is released and migrates to another enzyme, which restores and releases the original reduced/oxidized form and thus closes the catalytic cycle. The couple NAD⁺/NADH is often involved in catabolic reactions acting as an oxidizing agent, for example, for the formation of carbon acids from aldehydes, or aldehydes and ketones from alcohols, whereas the pair NADPH/NADP⁺ frequently serves as a reducing agent in anabolic reactions building up larger molecules, for example, during photosynthesis, that is, the formation of sugars from carbon dioxide and light. A systematic analysis of enzyme–coenzyme complexes revealed, that the NADP coenzymes are more flexible in conformation than those of NAD, and that the NADP protein interactions are quite variable compared to those of NAD.^[3]

Although the by far highest interest in NAD(P)H/NADP⁺ is due to its role as a coenzyme, which is to a large extent determined

by the hosting enzyme, there is also some interest in the compound as such. NAD(P)H and its derivatives are known to play vital roles in antioxidation and reductive biosynthesis.^[4–6] They also have been shown to be involved in physiological functions such as aging, oxidative stress, ROS (reactive oxygen species) production, cell death, and so on. Due to the high cost of NAD(P)H, numerous strategies have been tested for its in situ regeneration.^[7] Crystal structures of compact NAD(P), with a stacking of the nicotinamide and adenine moieties, as well as several extended forms, all bound to enzymes, are available.^[8] An equilibrium between folded (55%) and unfolded (45%) NADH in methanol was investigated by fluorescence excitation transfer spectroscopy.^[9] Two characteristic differences between NADPH and NADP⁺ are worthwhile to mention. It was found that NADPH

[a] X. Cao, L. Wu, M. Dolg

Institute for Theoretical Chemistry, University of Cologne, Greinstr. 4, D-50939, Cologne, Germany
E-mail: x.cao@uni-koeln.de or m.dolg@uni-koeln.de

[b] L. Wu

Key Laboratory of Theoretical and Computational Photochemistry of Ministry of Education, Department of Chemistry, Beijing Normal University, Xin-wai-da-jie No. 19, Beijing 10087, China

[c] J. Zhang

Department of Chemistry, University of Illinois at Urbana Champaign, Urbana, Illinois, 61801-3364

Contract Grant sponsor: Deutsche Forschungsgemeinschaft; Contract Grant number: CA 1390/1-1

This is an open access article under the terms of the Creative Commons Attribution License, which permits use, distribution and reproduction in any medium, provided the original work is properly cited.

© 2019 The Authors. *Journal of Computational Chemistry* published by Wiley Periodicals, Inc.

is stable in base but labile in acid, whereas the oxidized form NADP⁺ is stable in acid but labile in base.^[7] Moreover NADPH absorbs light at a wavelength of 340 nm, while NADP⁺ does not.^[10] Although much experimental work has been done to study the spectral properties of NAD(P)H,^[11,12] theoretical studies using a first-principles approach are still very limited. In 2007, De Ruyck and coworkers^[10] published results for fragments representing the π -conjugated groups of NADPH/NADP⁺ calculated at the density functional theory (DFT) level. Their calculations properly reproduce the aromatic/quinoidic character of NADPH/NADP⁺, as well as the maximal absorption wavelength of the conjugated moieties in both their oxidized and reduced forms. However, the geometric and electronic structures of the complete NADPH/NADP⁺ molecules, their ultraviolet–visible (UV–vis) spectra, as well as the reaction mechanism for the oxidation of NADPH to NADP⁺ are still missing.^[10]

In the present work, we report the first systematic quantum chemical study of NADPH/NADP⁺ at the DFT level. The geometric and electronic structures as well as the UV–vis spectra of NADPH/NADP⁺ in gas phase and aqueous solution were both calculated by using different density functionals. NADPH.100H₂O and NADP⁺.100H₂O complexes combined with the polarizable continuum model (COSMO) have been used to model NADPH and NADP⁺ in aqueous solution, respectively. Moreover, the oxidation of NADPH to yield NADP⁺ under aerobic conditions in acidic solution has also been investigated.

Methods

The electronic structure calculations were carried out with the TURBOMOLE^[13] program package unless otherwise noted. The computational method was DFT using the semi-empirical gradient-corrected exchange–correlation three-parameter hybrid density functional approach B3LYP,^[14–17] the PBE^[18,19] functional, that includes 25% of exact exchange, as well as the pure generalized gradient approximation (GGA) type density functional BP86.^[14,20] Selected minimum structures resulting from geometry optimizations were confirmed by frequency calculations. Calculations taking into account bulk solvent effects were carried out using COSMO (conductor-like screening model),^[21] a kind of dielectric continuum model. For the cavity generation the following atomic radii (Å) were used in our calculations: C (2.0), N (1.83), O (1.72), H (1.3) and P (2.106). For all other parameters the default values implemented in TURBOMOLE were adopted. The standard def-SV(P) and def2-TZVP basis sets were applied, that is, def-SV(P): H(4s)/[2s],^[22] P (10s7p1d)/[4s3p1d]^[23] and C, O, N (7s4p1d)/[3s2p1d]^[23] (denoted as basis sets A hereafter); def2-TZVP: H (5s1p)/[3s1p], P: (14s9p3d1f)/[5s5p2d1f]^[24] and C, O, N (11s6p2d1f)/[5s3p2d1f]^[24] (denoted as basis sets B hereafter).

The crystal structures of NADPH^[10,25] including compact and extended forms were taken as an initial guess for geometry optimizations of NADPH/NADP⁺ in the gas phase using basis sets A and B. The molecular structures of NADPH and NADP⁺ in aqueous solution were then determined starting from both the compact and the extended gas phase conformers with the lowest energies. First 100 water molecules were located around the

optimized gas phase structures of NADPH/NADP⁺ in a manner of spherical layers by using the software PACKMOL^[26]; thereafter the obtained geometries of NADPH.100H₂O/NADP⁺.100H₂O were optimized at semi-empirical level by using the software XTB (an extended tight-binding semi-empirical program package)^[27]; finally the obtained structure of the second step was optimized again with TURBOMOLE^[13] at the DFT level using basis sets A. Due to the limit of our computational facilities we were unable to perform such calculations for NADPH.100H₂O and NADP⁺.100H₂O using the larger basis sets B. It is clear that with the outlined procedure it is unlikely to find the global minimum of NADPH/NADP⁺ in aqueous solution; however, it is possible to account for the most important structural changes due to hydration, for example, replacement of intramolecular by intermolecular hydrogen bonds and partial deprotonation.

As an alternative to the above procedure we applied a Monte Carlo conformer search using the Merck molecular force field (MMFF94s)^[28,29] as implemented in the software OPEN BABEL.^[30] Originating from four starting conformers a total of about 4×10^4 conformers were generated. The lowest energy structures for every 100 subsequently generated conformers were further optimized using the tight binding code XTB,^[27] resulting in 4×100 gas phase structures. Of these about 11 structures each of NADPH and NADP⁺ were further optimized in the gas phase at the BP86 and B3LYP level, including at least five with a configuration corresponding to naturally occurring NADPH and NADP⁺. Thereafter, spherical layers of 100 water molecules were added to the gas phase structures using PACKMOL^[26] and the resulting systems were again optimized with the tight binding package XTB,^[27] this time including also contributions of dispersion interaction and bulk water. The three energetically lowest structures corresponding to naturally occurring NADPH were further optimized with TURBOMOLE^[13] using the BP86 and B3LYP density functionals, the D3 dispersion correction,^[31] and basis sets A. The final energies were obtained by adding the zero-point vibrational energy and including bulk water contributions with COSMO.^[21] Similar calculations were performed to test the stability of the results for a larger number of explicitly treated water molecules, that is, 150.

In the above described procedure not only conformers of NADPH and NADP⁺ were obtained, but also stereoisomers of these, which to our knowledge do not occur in nature. These mainly result from a replacement of the D- β -ribofuranose by one of its stereoisomers. For some energetically low-lying structures the corresponding naturally occurring forms of NADPH and NADP⁺ could be reestablished by changing the configuration at the furanose carbon centers by hand. Moreover, the orientation of the acid amide group in the nicotinamide moiety was also changed by hand to possibly obtain another low-energy structure. In the following, we denote as *cis* when the oxygen of the acid amide group and the N atom of the pyridine ring are on the same side, and as *trans* when they are on opposite sides. We use labels such as, for example, **1a_c** and **1a_t** for the *cis* and *trans* conformers, respectively, of otherwise similar structures and **1a** to denote both. Odd numbers denote NADPH, even ones NADP⁺; **1** and **2** refer to the gas phase, **3** and **4** to the solution.

The UV–vis absorption spectra of NADPH, NADP⁺, NADPH.100H₂O and NADP⁺.100H₂O were obtained by treating the electronic excitations within the adiabatic approximation of time-dependent density functional theory (TD-DFT). Between 200 and 500 energetically lowest singlet–singlet excitations were calculated, covering the range of the experimentally recorded UV–vis spectra (220–400 nm).^[10] For every calculated spectral line *i* one Gaussian function $f_i \exp(-b(\lambda - \lambda_i)^2)$ was used to represent the contribution to the spectrum. Here f_i is the calculated oscillator strength (length representation), λ_i is the calculated wavelength, and *b* is a broadening parameter, which is taken as 0.05 for the gas phase and 0.005 for the aqueous solution. The continuous spectrum in a given interval was obtained pointwise, as the sum over the up to 500 Gaussian functions, for each wavelength λ . The reported band maxima λ_{max} and intensities were determined from the continuous spectra.

For the hydrogen transfer reaction involved in the oxidation of NADPH by singlet oxygen, that is, NADPH + ¹O₂ → NADP⁺ + HO₂⁻, the geometry of NADPH optimized at the DFT/BP86 level by using basis sets B was taken and ¹O₂ was added. The potential energy curve of the system was scanned with respect to the distance between the atom H and one O of O₂ at the DFT/BP86 level by using basis sets A. In order to check if a single electron transfer prior to the hydrogen transfer from NADPH to ¹O₂ occurs, the triplet and singlet states of the reactants were calculated at the state-averaged CASSCF level, in which a total CAS(8e,5o) active space was used. The final energies of the triplet state corresponding to NADPH⁺ + ¹O₂⁻ and the singlet state corresponding to NADPH + ¹O₂ were obtained from MRCI//CASSCF(6,4)/def2-SV(P) calculations, in which all orbitals with energies below -0.5 au were put into the core. All MRCI//CASSCF computations were carried out with the MOLPRO program package.^[32–35] Cartesian coordinates of the energetically lowest structures of NADP⁺/NADPH in gas phase and solution are provided for B3LYP in the supplementary material.

Results and Discussion

Structures and relative stabilities

NADPH/NADP⁺ in gas phase. NADPH (C₂₁H₃₀N₇O₁₇P₃) contains 78 atoms and can be viewed as a system composed of the two terminal adenine and nicotinamide ring systems, linked by a flexible chain made of a D-β-ribofuranose-dihydrogenphosphate, a dihydrogenpyrophosphate and a D-β-ribofuranose unit. Each of these moieties can participate in intramolecular hydrogen bonding in multiple ways, that is, there are totally 18 hydrogen bond acceptors, 9 hydrogen bond donors and 13 rotatable bonds.^[36] Since the unit linking the terminal ring systems contains already 10 rotatable bonds a large number of conformers is possible, for example, we found local minima for compact structures with a direct interaction between the terminal ring systems (rings either stacked or paired in a coplanar arrangement), curled structures where both rings interact with the linking unit but not with each other, partially curled structures with only one ring interacting

with the linking unit as well as extended structures where the rings are not involved in interactions. Due to the multiple possibilities of hydrogen bonding within the linking unit a large variety of these structural motifs is possible (cf. the supporting information for selected XTB gas phase structures).

Aside from hydrogen bonding also intramolecular proton transfer increases the variety of possible structures. Adenine is one of the four nucleobases of DNA. The preferred protonation positions in order of decreasing stability are the ring N atoms 1, 3 and 7.^[37] Since strongly acidic dihydrogenphosphate and dihydrogenpyrophosphate groups are present in NADPH/NADP⁺, a proton transfer can occur. Moreover, acid amides are known to behave as weak bases. Using BP86 and B3LYP together with basis sets B we calculated the proton affinity of nicotinamide for a protonation of the O in the acid amide group to be ≈866 kJ/mol, the one of dihydronicotinamide to be ≈933 kJ/mol. These values are quite close to our corresponding calculated value for adenine of ≈942 kJ/mol, which is in excellent agreement with experimental data (942.8 kJ/mol)^[38] and other theoretical results from the literature.^[37,39,40] In several low-lying gas phase structures of NADPH/NADP⁺ we found in fact a protonation of a ring nitrogen in the adenine moiety or the oxygen in the nicotinamide group. Usually these tautomeric structures result from the switching of the roles of proton donor and acceptor in hydrogen bonds between a terminal ring and the bridging unit, for example, P–O–H···O=C → P–O(–)···H–O–C(+) or P–O–H···N → P–O(–)···H–N(+). In case of the nicotinamide this resembles the intermediate structure in a first step of an acid amide hydrolysis in an acidic medium; however, in case of nicotinamide the positive charge is not fixed on the acid amide carbon atom (which would allow the nucleophilic attack by a water molecule in the hydrolysis), but is delocalized over the adjacent ring system. Similarly, the positive charge on the ring nitrogen is delocalized over the adenine moiety. This intramolecular proton transfer thus leads to stable zwitterionic tautomers of NADPH/NADP⁺, which often maintain the hydrogen bond with the changed polarity.

B3LYP, PBE0 and BP86 yield quite similar NADPH and NADP⁺ gas phase structures (Fig. 1). The maximum deviations of the B3LYP (PBE0) and BP86 interatomic distances (with up to 1.5 times the sum of covalent radii) of the energetically lowest NADPH structures **1a_c–1e_c** and **1a_t–1c_t** in Å are C–C 0.022 (0.030), C–N 0.018 (0.022), C–O 0.023 (0.027), O–P 0.032 (0.037), C–H 0.013 (0.012), N–H 0.032 (0.020), O–H 0.082 (0.069), where the larger value for O–H is related to the different extent of hydrogen bond formation. In almost all cases the B3LYP (PBE0) distances are shorter than the BP86 ones. As a measure of the extent of folding or the compactness of the system we consider the average distance *C* between any two non-hydrogen atoms in the system. For **1a_c–1e_c** and **1a_t–1c_t** the B3LYP (PBE0) values are on average only 0.02 (0.04) Å larger (smaller) than the BP86 results.

The relative energies of the lowest conformers of NADPH and NADP⁺ in the gas phase are listed in Table 1. The values discussed in the following include the zero-point vibrations. For NADPH structure **1a_t** (C: BP86 6.39 Å, B3LYP 6.42 Å, PBE0 6.39 Å) has the lowest energy for all three density functionals

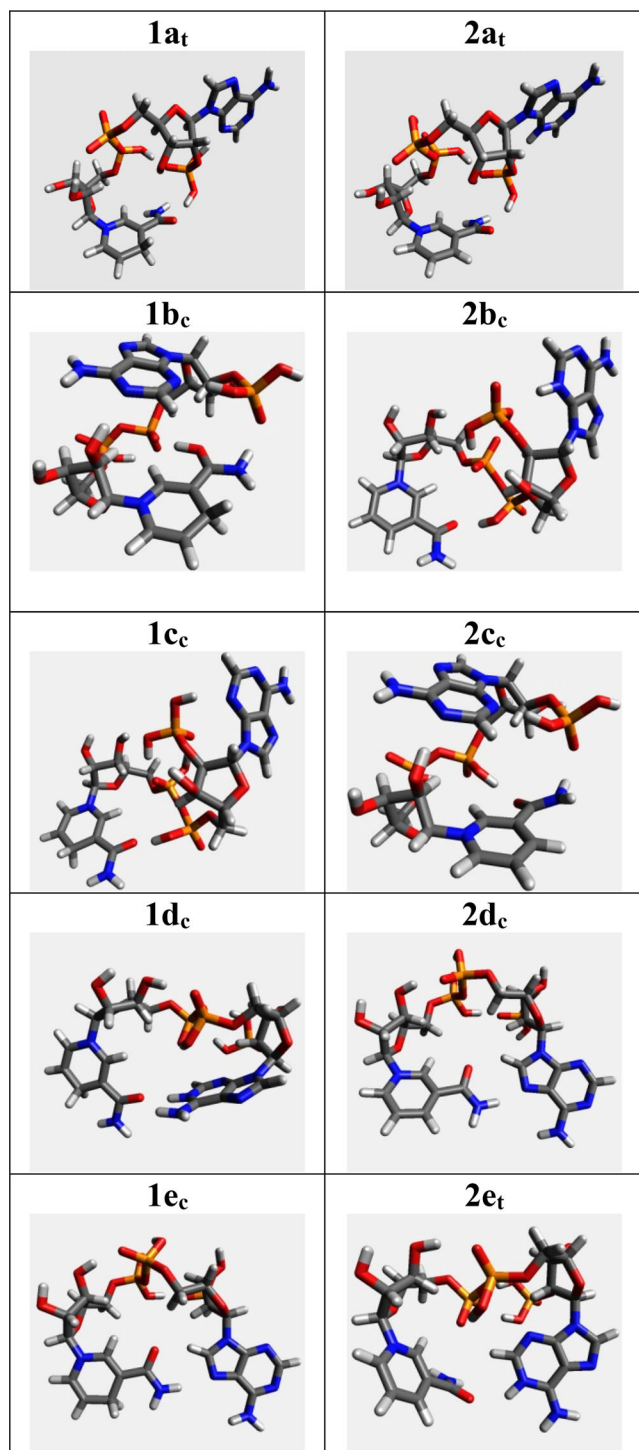


Figure 1. Optimized structures of NADPH and NADP⁺ in gas phase using basis sets B at the DFT/B3LYP level. Only the lower one of the *cis* and *trans* conformers of **1a–1e** and **2a–2e** is shown. The BP86 and PBE0 structures are very similar. Relative energies see Table 1. [Color figure can be viewed at wileyonlinelibrary.com]

applied here. Whereas the adenine ring system is essentially free and interacts only by one hydrogen bond between a ring N atom and a O–H group of the phosphate unit, the nicotinamide moiety forms a hydrogen bridge bond between the N atom of the acid amide group and a O–H group of the

pyrophosphate unit, leading to the formation of a ring on this side of NADPH and a partly curled structure. The ordering of the other low-energy structures **1a_c**, **1b_c**, **1b_t** and **1c_c** depends on the density functional.

Structure **1b_c** is quite low in energy at the B3LYP (2.8 kJ/mol) and PBE0 (3.0 kJ/mol) level, but substantially higher at the BP86 level (15.7 kJ/mol). It is of a cage-like compact form (C: BP86 5.59 Å, B3LYP 5.65 Å, PBE0 5.58 Å) stabilized by six (B3LYP, PBE0) to eight (BP86) hydrogen bonds. The two terminal ring systems reside in approximately parallel planes at a distance of about 4 Å, but are not stacked. The dihydro nicotinamide moiety is involved in two hydrogen bridge bonds: one between the NH₂ unit of the acid amide group (donor) and the P=O unit of the dihydrogenphosphate group on the D-β-ribofuranose (acceptor) and one between the protonated C=O unit of the acid amide group, C–O–H (donor), and the deprotonated P–O–H unit of the dihydrogenpyrophosphate group, P=O (acceptor). Attempts to obtain a (local) minimum structure with the expected hydrogen bond C=O···H–O–P by shifting the H atom and performing a reoptimization, always led to the structure described above. The adenine moiety takes part in three hydrogen bonds at the BP86 level: the NH₂ group (donor) interacts with a C–O–H unit on the unsubstituted D-β-ribofuranose (acceptor), and the two nitrogen atoms in the six-membered ring (acceptors) interact with a P–O–H unit of the dihydrogenphosphate group on the D-β-ribofuranose (donor) and a C–O–H unit on the unsubstituted D-β-ribofuranose (donor). At the B3LYP and PBE0 level the NH₂ group of the adenine is not involved in hydrogen bonding. Two (B3LYP, PBE0) or three (BP86) additional hydrogen bonds within the bridging units stabilize these three structures, which are quite similar, but not entirely identical.

Structures **1b_t** (C: BP86 5.62 Å, B3LYP 5.62 Å, PBE0 5.55 Å) and **1a_c** (C: BP86 6.44 Å, B3LYP 6.45 Å, PBE0 6.39 Å) are close to each other in energy and reside about 10–13 kJ/mol above the lowest structure **1a_t** for all three density functionals. Their overall shape is closely related to the ones of **1b_c** or **1a_c**, with only small differences in the arrangements of the hydrogen bridge bonds at the nicotinamide moiety. The structures **1c_c** (C: BP86 6.41 Å, B3LYP 6.47 Å, PBE0 6.35 Å) have relative energies of 8–20 kJ/mol. They show only one hydrogen bond from each of the terminal rings to the linking unit. All functional groups are as expected, that is, no changes of donor and acceptor in hydrogen bonds is observed. The related structures **1c_t** (C: BP86 6.55 Å, B3LYP 6.55 Å, PBE0 6.45 Å) are found at significantly higher energies, since the strong hydrogen bond between the nicotinamide oxygen atom and a –OH group on the pyrophosphate unit in **1c_c** is replaced by a weaker interaction between the nicotinamide –NH₂ group and an oxygen atom on the pyrophosphate in **1c_t**.

An interesting structure (**1d_c**) is found at somewhat higher energy (BP86 53.1 kJ/mol, B3LYP 45.5 kJ/mol, PBE0 49.4 kJ/mol): the terminal rings are located in orthogonal planes and interact directly by means of hydrogen bonding, leading to a relatively compact structure (C: BP86 5.98 Å, B3LYP 5.97 Å, PBE0 5.93 Å). Involved as hydrogen bond donor are the amino group on the adenine and the nearby protonated ring N atom at position

Table 1. Relative energies (kJ/mol) of low-energy conformers of NADPH and NADP⁺ in the gas phase from BP86, B3LYP and PBE0 calculations. Values in parentheses are corrected for zero-point vibration (cf. Fig. 1 for structures **1a–1e** and **2a–2e**).

	NADPH			NADP ⁺			
	BP86	B3LYP	PBE0	BP86	B3LYP	PBE0	
1a_c	3.6 (11.0)	6.3 (11.1)	5.8 (11.4)	2a_c	39.7 (41.9)	42.3 (43.9)	44.3 (45.7)
1a_t	0.0 (0.0)	0.0 (0.0)	0.0 (0.0)	2a_t	0.0 (0.0)	0.0 (0.0)	0.0 (0.0)
1b_c	11.0 (15.7)	4.6 (2.8)	3.3 (3.0)	2b_c	48.9 (49.8)	46.1 (44.0)	51.0 (50.3)
1b_t	3.1 (12.9)	5.2 (11.1)	3.5 (10.3)	2b_t	24.8 (26.3)	19.0 (18.0)	24.3 (24.5)
1c_c	18.7 (19.5)	10.0 (8.3)	14.9 (14.4)	2c_c	60.9 (58.2)	56.3 (51.9)	58.1 (55.1)
1c_t	63.0 (63.5)	51.7 (48.5)	59.5 (57.9)	2c_t	108.9 (110.8)	92.3 (89.0)	96.9 (95.6)
1d_c	43.3 (53.1)	39.3 (45.5)	42.1 (49.4)	2d_c	76.3 (73.1)	68.2 (63.1)	74.8 (70.3)
1d_t	61.8 (72.0)	60.2 (66.1)	63.0 (70.6)	2d_t	91.6 (87.8)	86.1 (79.3)	94.4 (88.4)
1e_c	60.6 (65.9)	47.1 (47.0)	56.3 (58.2)	2e_t	93.3 (98.6)	83.3 (85.6)	88.5 (92.3)

Basis sets B.

1, whereas the C=O unit of the nicotinamide is the hydrogen bond acceptor. Another structure (**1e_c**) with a direct interaction between the rings (BP86 65.9 kJ/mol, B3LYP 47.0 kJ/mol, PBE0 58.2 kJ/mol) results from the optimization of an experimental X-ray structure. In this not very compact structure (C: BP86 6.36 Å, B3LYP 6.38 Å, PBE0 6.31 Å) the two ring systems occupy a common plane and interact by means of hydrogen bonding.

NADP⁺ is formally obtained from NADPH by removal of a hydride ion from the nicotinamide moiety. The energetically lowest structures of NADP⁺ are closely related to those of NADPH (Fig. 1); however, the energetic order has been drastically changed (Table 1). As for NADPH the B3LYP results for NADP⁺ structures and relative energies roughly agree with the BP86 and PBE0 ones. The maximum deviation between B3LYP (PBE0) and BP86 bond distances in Å are C–C 0.012 (0.018), C–N 0.013 (0.023), C–O 0.016 (0.027), O–P 0.023 (0.029), C–H 0.011 (0.008), N–H 0.029 (0.019), O–H 0.049 (0.040), again with B3LYP (PBE0) yielding usually shorter bond distances than BP86. The B3LYP and BP86 measures for the compactness C averaged for **2a_c–2d_c**, **2a_t–2c_t** and **2e_t** agree within 0.01 Å, whereas the values are on average 0.07 Å smaller for PBE0.

In contrast to NADPH there is one structure of NADP⁺ which is significantly (by 18 kJ/mol or more) lower in energy than all others investigated here, that is, conformer **2a_t** (C: BP86 6.35 Å, B3LYP 6.35 Å, PBE0 6.29 Å) which has a curled shape on the nicotinamide side and resembles closely the lowest NADPH conformer **1a_t**. The related conformer **2a_c** (C: BP86 6.43 Å, B3LYP 6.44 Å, PBE0 6.38 Å) is located 42–46 kJ/mol higher in energy and roughly corresponds to the low-energy naturally occurring NADPH conformer **1a_c**, except that a switch of proton donor and acceptor occurred in two hydrogen bonds, that is, one between the N at position 3 in adenine and the dihydropyrophosphate unit and one between the O in nicotinamide and the dihydropyrophosphate unit. One of the two protons of the dihydropyrophosphate unit is either transferred to the O of the nicotinamide (NADPH **1a_c**) or to the N of the adenine (NADP⁺ **2a_c**).

For the conformers **2b_c** and **2b_t** with relative energies of 18–50 kJ/mol the *trans* form of the nicotinamide is also always clearly lower in energy, that is, by 20–26 kJ/mol, than the *cis* form. Structure **2b_t** of NADP⁺ (BP86 26.3 kJ/mol, B3LYP 18.0 kJ/mol, PBE0 24.5 kJ/mol) corresponds to the NADPH structure **1c_t**. In contrast to the latter a proton is transferred from the

dihydrogenphosphate group to the adenine, thus leading to a change of donor and acceptor in the corresponding hydrogen bond (C: BP86 6.41 Å, B3LYP 6.41 Å, PBE0 6.33 Å). Structure **2c_c** (BP86 58.2 kJ/mol, B3LYP 51.9 kJ/mol, PBE0 55.1 kJ/mol) is related to NADPH structure **1b_c**; however, the change of donor and acceptor in the hydrogen bond between the O in nicotinamide and dihydrogenphosphate is not observed (C: BP86 5.67 Å, B3LYP 5.66 Å, PBE0 5.59 Å).

As for NADPH the two next higher structures of NADP⁺ exhibit a direct interaction between the terminal rings by means for hydrogen bonds, but are in different energetic order. Structure **2d_c** (BP86 73.1 kJ/mol, B3LYP 63.1 kJ/mol, PBE0 70.3 kJ/mol) features paired terminal rings in a common plane (C: BP86 6.39 Å, B3LYP 6.40 Å, PBE0 6.35 Å), as does the NADPH structure **1e_c**. The arrangement of the terminal rings in nearly orthogonal planes in the NADPH structure **1d_c** is lost in the NADP⁺ structure **2e_t** (BP86 98.6 kJ/mol, B3LYP 85.6 kJ/mol, PBE0 92.3 kJ/mol), but the proton transfer from the dihydropyrophosphate group to the N atom in position 1 of the adenine was maintained (C: BP86 5.92 Å, B3LYP 5.93 Å, PBE0 5.86 Å). Finally, it is fair to state that besides the gas phase structures of NADPH and NADP⁺ discussed here probably other energetically low-lying ones can be constructed, for example, by modifying locally the arrangement of some hydrogen bonds without destroying the overall connectivity. This remark is also true for the studies of NADPH in solution.

NADPH/NADP⁺ in aqueous solution. In the XTB calculations with explicitly treated water molecules NADPH also often undergoes deprotonation, but now an intermolecular proton transfer and the formation of H₃O⁺ ions is preferred. The weakly basic acid amide group frequently stays intact, whereas the protonation of the stronger nucleobase adenine occurs more frequent. We find that up to 4 H⁺ are removed from the P–O–H groups (two from the dihydrogenphosphate at the ribofuranose and two from the dihydropyrophosphate moiety), in agreement with the physiological charge of –4.^[36]

Adding 100 or more water molecules explicitly leads to a for all practical purposes uncountable number of structural possibilities, at least far too many to account for them at the DFT level. Therefore, we do not claim that we have located the absolute minima in our calculations, but we merely consider

the found structures as representatives of a large number of other energetically low-lying ones. According to our observation intramolecular hydrogen bonding within NADPH/NADP⁺ is partly replaced by intermolecular hydrogen bonding between NADPH/NADP⁺ and water, often leading to less compact structures (cf. supporting information for selected XTB/DFT structures in gas phase and solution). Another observation is that the explicitly treated water molecules tend to avoid the π systems of the terminal rings, so that these are either located in a cavity of the water network or after geometry optimization end up at the surface of the water-NADPH/NADP⁺ droplet (cf. Fig. 2). Although the explicitly treated water molecules do not surround NADP⁺/NADPH completely, the influence of bulk water is still accounted for by the COSMO treatment.

Due to the large computational effort (up to 10³ geometry optimization steps, 2544 and 3444 contracted basis functions for basis set A with 100 and 150 water molecules, respectively), despite the use of smaller basis sets and the RI technique, only a couple of structures were further optimized at the BP86 and B3LYP levels. Initial guesses were taken from the gas phase structures lowest in energy as well as from crystal data. The resulting low-energy structures for BP86 and B3LYP look quite similar, but are sometimes in a different energetic order. It should be noted that hydrogen bonding between the explicitly treated water molecules and the bulk water is not modeled accurately by COSMO. Considering the large number of unpaired hydrogen bond donors and acceptors at the surface of the explicitly treated droplet of 100 water molecules and the strength of one O—H...O bond of ≈ 20 kJ/mol, differences in relative stabilities of several tens of kJ/mol can result also from the inaccurate treatment of these hydrogen bonds and not only

from the NADPH/NADP⁺ conformer and its interaction with the surrounding water molecules. We thus discuss only the lowest structures which are common to B3LYP and BP86, three of which are depicted in Figure 2, and differ in their relative energies by not more than the strength of two hydrogen bonds.

The relative energies discussed in the following include the dispersion interaction estimate (D3) due to Grimme, the zero-point vibration correction for NADPH/NADP⁺ and the 100 explicitly treated water molecules as well as the bulk water effects accounted for by COSMO.

The lowest energy structure at the B3LYP level (**3a_t**) is completely uncurled (C: BP86 7.71 Å, B3LYP 7.72 Å). Essentially all intramolecular hydrogen bonds were replaced by intermolecular ones. The NADPH is threefold deprotonated, that is, one proton less than corresponding to the physiological charge of -4 ,^[36] to form H₃O⁺ ions with the explicitly treated water molecules. In the gas phase extended structures corresponding to **3a_t** have relative energies far above 100 kJ/mol. The same holds for the corresponding *cis* conformer **3a_c**, which is slightly more extended (C: BP86 7.94 Å, B3LYP 7.96 Å) and 31.5 kJ/mol higher in energy.

A partly curled structure (**3b_t**) is located at 13.0 kJ/mol at the B3LYP level. It is only slightly less compact (C: BP86 6.48 Å, B3LYP: 6.50 Å) than the gas phase structures studied here (C: BP86 5.59–6.44 Å, B3LYP 5.65–6.47 Å). The adenine ring system does not interact with the rest of the NADPH molecule, whereas the amino moiety of the amide group forms a hydrogen bond to the twofold deprotonated dihydrogenphosphate on the ribofuranose. Thus, the nicotinamide side of NADPH is curled, or in other words the nicotinamide, the two ribofuranose units and the bridging twofold deprotonated dihydrogenpyrophosphate

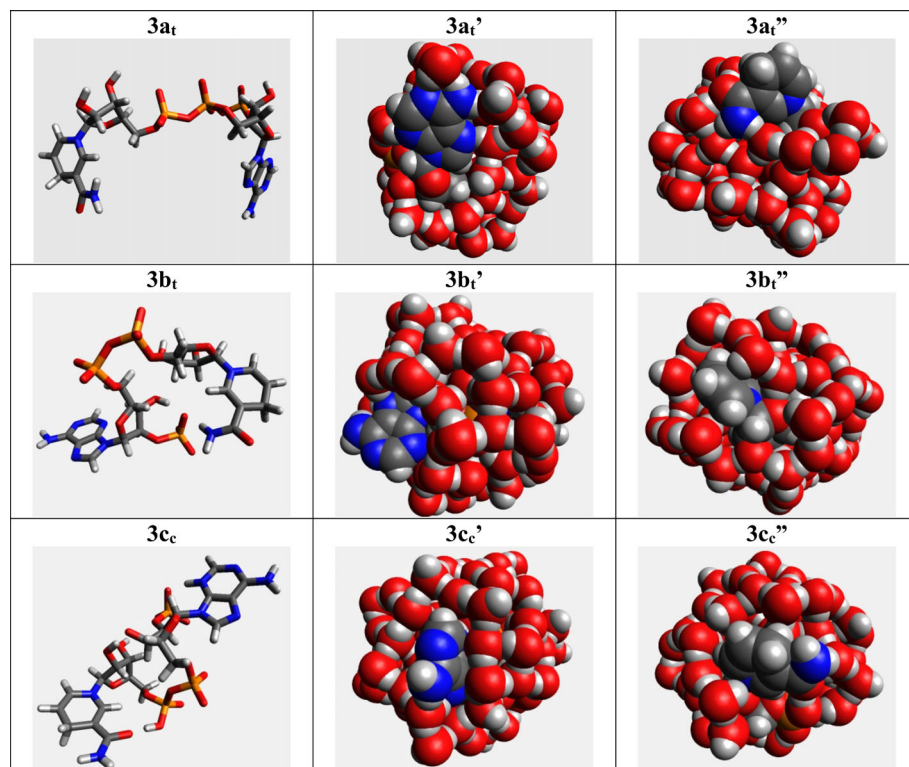


Figure 2. Partly deprotonated NADPH moieties from the energetically lowest structures of NADPH+100 H₂O at the B3LYP + D3 + COSMO + OC + ZPE level using basis set A. Only the lower one of the *cis* and *trans* conformers of **3a–3c** is shown. The BP86 structures are very similar. The van der Waals spheres plots show the sides of the water droplet with the adenine and nicotinamide moieties. Relative energies see Table 4. [Color figure can be viewed at wileyonlinelibrary.com]

form a large ring. Here NADPH is fourfold deprotonated, in agreement with the physiological charge of -4 . The related *cis* conformer is even more compact (C: BP86 6.16 Å, B3LYP 6.21 Å) and slightly higher in energy (27.8 kJ/mol).

The next higher structure **3c_c** (29.4 kJ/mol) resembles the third lowest NADPH gas phase structure (**1c_c**), but is slightly less compact (C: BP86 6.48 Å, B3LYP 6.28 Å). As in the gas phase both the adenine and the nicotinamide side form only one hydrogen bond each to the middle part of the molecule. The hydrogen bond between the adenine ring N and the former dihydrogenphosphate on the ribofuranose exhibits a hydrogen transfer from O to N. All other protons on the dihydrogenphosphate and the pyrofuranose groups were removed to form H₃O⁺ ions, resulting in a NADPH charge of -3 . The related *trans* conformer is more compact (C: BP86 6.07 Å, B3LYP 6.10 Å) and higher in energy (54.1 kJ/mol). Although the B3LYP and BP86 structures are very similar, their relative energies differ significantly, also leading to a different energetic order. Nevertheless, both methods yield **3a_c** as the energetically lowest NADPH structure in solution.

The structures of NADP⁺ in solution were optimized starting from the low-energy solution structures of NADPH after removing one H⁻ from the nicotinamide ring. The obtained structures closely resemble the ones of NADPH, but the energetic order is different. In addition, the NADP⁺ structures **4a–4c** differ by less than 15 kJ/mol in energy, whereas the corresponding structures **3a–3c** of NADPH are spread over 55 kJ/mol. The completely uncurled structure **4a_c** (C: BP86 7.81 Å, B3LYP 7.86 Å) is lowest in energy, and the slightly more compact *cis* conformer **4a_c** (C: BP86 7.71 Å, B3LYP 7.74 Å) is only 12.3 kJ/mol higher.

The partly curled structures **4b_c** (C: BP86 6.27 Å, B3LYP 6.30 Å) and **4b_c** (C: BP86 6.14 Å, B3LYP 6.18 Å) are nearly degenerated with relative energies of 8.4 and 8.5 kJ/mol, respectively. At only little higher relative energies of 11.8 and 13.4 kJ/mol are the structures.

4c_c (C: BP86 6.15 Å, B3LYP 6.18 Å) and **4c_c** (C: BP86 6.10 Å, B3LYP 6.05 Å). The loss of protons to the solution is fourfold for structures **4a** and **4b**, and threefold for structures **4c**, where an intramolecular hydrogen bond between the N in the adenine ring and the phosphate group is formed. Similar to NADPH the low-energy structures **4a–4c** of NADP⁺ are spread over only 23 kJ/mol at the B3LYP level, compared to 71 kJ/mol at the BP86 level. In addition to a different energetic ordering BP86 yields structure **4c_c** as the most stable one, with **4a_c** being the second lowest (23.0 kJ/mol).

Additional structures **3d_c** and **4d_c**, which resulted from a X-ray structure starting geometry similar to **1e_c** and **2d_c**, were found to be significantly higher in energy. In summary, the low-energy structures of NADPH and NADP⁺ obtained with an explicit treatment of surrounding water molecules tend to be less compact than those in the gas phase and are two- to fourfold deprotonated.

Cis and trans conformers. The stability of *cis* and *trans* conformations of 1,4-dihydronicotinamide (NH) and protonated nicotinamide (N⁺) in gas phase and solution was investigated with DFT by Russo and coworkers.^[41] It was found that in the gas

phase the *cis* conformation of the N atom in the pyridine ring and the O in the acid amide group is by about 8.7–15.9 and 6.7–9.7 kJ/mol more stable than the *trans* conformation for NH and N⁺, respectively. In aqueous solution, modeled by a continuum model, the *cis* conformation of N⁺ is more stable than the *trans* conformation by 12.0 kJ/mol, whereas for NH the *trans* conformation is more stable by 10.5 kJ/mol than the *cis* conformation. Experimental evidence exists, for example, for *Escherichia coli* dihydrofolate reductase that NADPH adopts a *trans* conformation in this enzyme.^[42] Since the protein pocket hosting NADPH/NADP⁺ is quite rigid, the above results suggest that the binding of NADP⁺ to the protein might be weaker than the one of NADPH. Feeney and coworkers actually found by ¹H/¹⁵N nuclear magnetic resonance (NMR) studies that the enzyme *Lactobacillus casei* dihydrofolate reductase binds about 1500 times tighter to NADPH than to NADP⁺ and performed DFT calculations on model systems for the protein-coenzyme interactions.^[43] The pronounced difference of the binding strength was explained by the necessary change from the *cis* to the *trans* conformation for NADP⁺ when binding to the protein, whereas NADPH already exists (mainly) in the *trans* conformation in solution.

Our calculations on the *cis* and *trans* conformers of 1,4-dihydronicotinamide and protonated nicotinamide confirm the gas phase results of Russo and coworkers, for example, the B3LYP results agree within 0.3 kJ/mol. The *cis* conformers are more stable than the *trans* forms by 8.5 (8.9) and 6.1 (6.4) kJ/mol at the BP86 (B3LYP) level including zero-point vibration corrections for 1,4-dihydronicotinamide and protonated nicotinamide, respectively. However, when modeling hydration with the COSMO approach we do not find a reversal of the stability for protonated nicotinamide, but only a significant lowering of the relative energy of its *trans* conformer. The energies of the *trans* conformers relative to the *cis* forms including zero-point vibration corrections are 7.2 (8.6) and 1.9 (1.9) kJ/mol at the BP86 (B3LYP) level for 1,4-dihydronicotinamide and protonated nicotinamide, respectively. We attribute this difference mainly to the shape of the cavity used in the continuum solvation model. Russo and coworkers used a single sphere, which might not be as appropriate for nonspherical molecules as the cavity constructed from atom-centered spheres within the COSMO approach. Due to the numerous possibilities to form intra- and intermolecular hydrogen bonds the picture becomes less clear when instead of the model systems NADPH and NADP⁺ are considered. In the gas phase there are several NADPH conformers, both *cis* (**1b_c**) and *trans* (**1a_c**), with a relatively low energy, whereas for NADP⁺ a single *trans* conformer (**2a_c**) is significantly more stable than the others. In aqueous solution both for NADPH and NADP⁺ a *trans* conformer is lowest in energy (**3c_c**, **4c_c**). However, whereas for NADP⁺ both *cis* and *trans* conformers exist at relative energies of less than 10 kJ/mol (**4a_c**, **4b_c**, **4b_c**), this is not the case for NADPH. Overall we obtain for both NADPH and NADP⁺ in the gas phase as well as in solution a *trans* conformer as lowest in energy (**3a_c**, **4a_c**). The explanation of the difference in binding strength of NADPH and NADP⁺ to a protein in an enzyme solely based on the stability of the *cis* and *trans* conformers at the nicotinamide moiety is only

Table 2. Wavelengths of absorptions (λ , nm) and corresponding oscillator strength (length representation; in parentheses) for the TDDFT/B3LYP UV-vis absorption spectra of the five energetically lowest naturally occurring NADPH stereoisomers in the gas phase (cf. Fig. 1 for **1a–1c**).

1a_c	1a_t	1b_c	1b_t	1c_c
C = 6.45 Å	C = 6.42 Å	C = 5.65 Å	C = 5.62 Å	C = 6.47 Å
355.9 (0.17)	355.1 (0.12)	349.2 (0.13)	371.7 (0.13)	341.8 (0.12)
249.7 (0.23)	249.8 (0.23)	251.9 (0.14)	257.6 (0.10)	250.0 (0.20)
235.7 (0.08)	235.5 (0.08)	240.9 (0.03)	211.9 (0.05)	237.4 (0.09)
223.1 (0.03)	211.2 (0.08)	240.5 (0.05)	209.4 (0.04)	214.8 (0.04)
206.5 (0.25)	205.3 (0.07)	210.1 (0.02)	208.4 (0.02)	200.3 (0.08)
204.3 (0.05)	201.3 (0.02)	202.5 (0.10)	204.7 (0.03)	200.0 (0.18)
201.4 (0.06)	200.8 (0.03)	201.5 (0.07)	200.4 (0.02)	198.6 (0.05)

Only the seven most intense transitions with wavelengths longer than ≈ 200 nm are listed. Basis sets B.

consistent with our calculations on model systems. It seems that for the real molecules NADPH and NADP⁺ also other conformational changes may play a role.

UV-vis absorption spectra

The calculated TDDFT/B3LYP wavelengths (λ , nm) and the corresponding oscillator strengths (f , arbitrary units) of the most intense UV-vis absorptions of five energetically low conformers of NADPH (**1a–1c**) and NADP⁺ (**2a–2c**) in the gas phase are listed in Table 2 and Table 3, respectively. Besides B3LYP we also performed calculations with the BP86 and PBE0 functionals. Whereas the PBE0 results are similar to the B3LYP ones, the BP86 results were found to be inferior. Since the pure GGA-type density functional BP86 does not include Hartree-Fock exchange in contrast to the hybrid density functionals B3LYP and PBE0, energetically higher occupied and lower virtual orbitals were obtained using BP86, leading to a general red shift of the BP86 UV-vis absorption maxima compared to the B3LYP and PBE0 results. For example, for the energetically lowest conformers of NADPH the 400 calculated singlet excitations cover the range from ≈ 460 to ≈ 160 nm in BP86, and from about ≈ 360 to ≈ 130 nm in B3LYP. A similar red shift of BP86 excitations compared to B3LYP ones was also observed for, for example, UV-vis absorption spectra of lanthanide (III) motexafins (Ln-Motex²⁺, Ln = La, Gd, Lu) in our previous studies,^[44] as well as for Pt(II) and Ir(III) complexes by Latouche et al.,^[45] or for small organic molecules by Caricato et al.^[46] In addition to the red shift we observe that the BP86 spectra exhibit more maxima/shoulders than the B3LYP and PBE0 spectra.

NADPH has 386 electrons, corresponding to 193 occupied orbitals in the ground state. The two highest occupied orbitals (HOMO) and the three lowest unoccupied orbitals (LUMO) are localized on one of the two terminal rings, that is, for **1a_t** on adenine (HOMO–1, LUMO, LUMO+2) and nicotinamide (HOMO, LUMO+1), and are of π -type (cf. Fig. 3 for HOMO and LUMO+1). The ordering of LUMO and LUMO+1 was found to depend on the molecular conformation. The other occupied orbitals next to the HOMO (HOMO–2, HOMO–3, etc.) are mixed contributions from lone pairs on oxygen atoms on the ribofuranose, the dihydrogenphosphate and the dihydrogenpyrophosphate. NADP⁺ has two electrons and one occupied orbital less than NADPH. The character and the energetic order of the orbitals relevant for the low-energy part of the UV-vis absorption spectra is similar to the ones of NADPH, that is, for **2a_t** the HOMO, LUMO+2 and LUMO+3 are localized on adenine, whereas LUMO and LUMO+1 are localized on nicotinamide. As for NADPH all these orbitals are of π -type. Again the occupied orbitals next to the HOMO have mainly oxygen lone-pair character and are mixtures with contributions from the ribofuranose, the dihydrogenphosphate and the dihydrogenpyrophosphate. The characteristic absorption peak near 350 nm of NADPH results for **1a_t** from the HOMO \rightarrow LUMO+1 transition located on nicotinamide (cf. Fig. 3), whereas the peak around 250 nm has a main contribution from the HOMO–1 \rightarrow LUMO, LUMO+2 transitions on adenine. An explanation of the main features of the UV-vis absorption spectrum of NADPH was provided in 2007 by De Ruycck et al.^[10] on the basis of TDDFT/PBE0 model calculations on the NADPH chromophoric fragments nicotinamide and adenine. The authors argued that the most notable

Table 3. Wavelengths of absorptions (λ , nm) and corresponding oscillator strength (length representation; in parentheses) for the TDDFT/B3LYP UV-vis absorption spectra of the five energetically lowest naturally occurring NADP⁺ stereoisomers in the gas phase (cf. Fig. 1 for **2a–2c**).

2a_c	2a_t	2b_c	2b_t	2c_c
C = 6.44 Å	C = 6.35 Å	C = 6.37 Å	C = 6.41 Å	C = 5.66 Å
261.4 (0.04)	334.2 (0.05)	260.3 (0.10)	259.2 (0.12)	254.8 (0.03)
250.4 (0.22)	251.6 (0.24)	252.2 (0.13)	251.1 (0.12)	254.7 (0.02)
237.9 (0.07)	236.0 (0.05)	235.1 (0.04)	234.5 (0.04)	241.5 (0.09)
233.7 (0.05)	229.1 (0.05)	234.7 (0.06)	231.4 (0.03)	236.7 (0.08)
219.6 (0.04)	221.9 (0.08)	213.8 (0.09)	230.9 (0.03)	218.4 (0.03)
219.2 (0.05)	209.9 (0.04)	209.8 (0.02)	212.3 (0.10)	208.7 (0.03)
210.9 (0.08)	207.8 (0.02)	207.7 (0.06)	208.7 (0.03)	206.0 (0.03)

Only the seven most intense transitions with wavelengths longer than ≈ 200 nm are listed. Basis sets B.

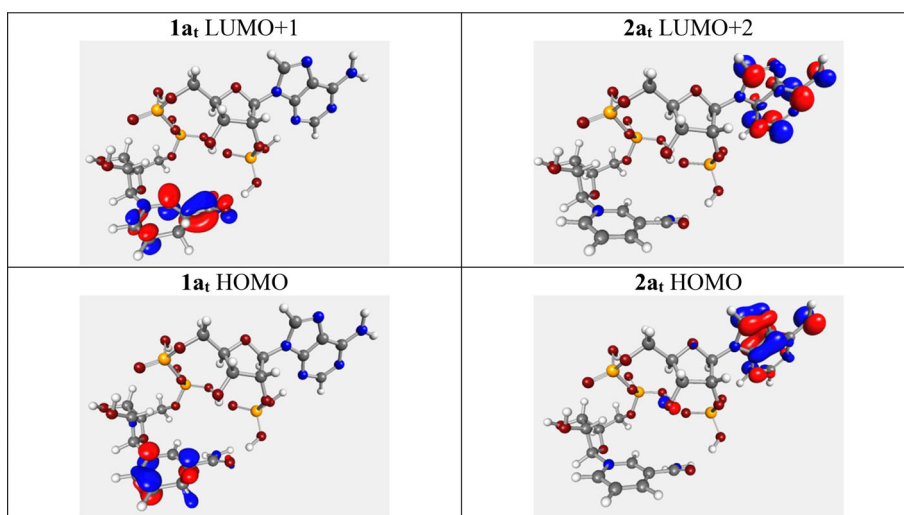


Figure 3. B3LYP Kohn-Sham orbitals involved in the characteristic transitions of NADPH (**1a_t**, 355.1 nm, HOMO → LUMO+1, 98.7%) and NADP⁺ (**2a_t**, 251.6 nm, HOMO → LUMO+2, 55.6%). [Color figure can be viewed at wileyonlinelibrary.com]

difference in the UV–vis spectra of NADPH and NADP⁺, that is, the absence of the characteristic peak near 350 nm in the latter, which is often used to detect NADPH/NADP⁺ in experiments,^[10] is related to the orbital stabilization by the positive charge of NADP⁺, which is mainly located on the ring of the nicotinamide moiety, and a corresponding increase of the gap between the relevant occupied and unoccupied orbitals compared to NADPH, for example, the HOMO–LUMO gap by about 1 eV. We note that the HOMO of NADPH becomes the LUMO of NADP⁺ (Fig. 3) and thus the transition around 350 nm occurring in NADPH on the nicotinamide is not possible in NADP⁺. Instead we find for NADP⁺ between 350 and 250 nm some peaks with low intensity resulting from transitions from the ribofuranose to the nicotinamide or the adenine. As for NADPH the maximum around 230–250 nm has a main contribution of an excitation on the adenine (HOMO → LUMO+2), compare Figure 3, whereas the lowest transition roughly localized only on nicotinamide is found near 210 nm.

The experimental absorption spectra for 0.1 mM aqueous solutions of pure NADPH/NADP⁺ were published by De Ruyck et al. in 2007.^[10] The spectra were recorded at room temperature under N₂ from 190 to 400 nm and featured a common absorption band centered at 259/260 nm for NADP⁺/NADPH. Based on the results of TDDFT/PBE0 calculations for the chromophoric fragments nicotinamide and adenine this common peak corresponds to the adenine moiety, which is present in both molecules. In addition, specific absorption bands centered around 220/340 nm were found for NADP⁺/NADPH and are related to the nicotinamide unit. The difference was explained by the strong stabilization of the occupied orbitals and the increase of the electronic gap due to the positive charge of NADP⁺, which is mainly localized on the nicotinamide six-membered ring. It should be noted that a specific absorption band around 220 nm for NAD(P)⁺ was not obtained in previous experimental work.^[47,48] The occurrence of a band at this wavelength for NAD(P)H in these studies might be due to contaminations by the oxidized form NAD(P)⁺, since De Ruyck et al. claim that they present the first study of “pure” NADPH.

The UV–vis spectra of NADPH.100H₂O (Fig. 4) and NADP⁺.100H₂O (Fig. 5) in bulk water modeled by COSMO were calculated with basis sets A. Besides the three low-energy structures **3a–3c** and **4a–4c** discussed above (see Fig. 3 for NADPH) we also include one resulting from the optimization of a crystal structure (see supporting information) related to **2d_c**. Our calculated TDDFT/B3LYP spectra for NADPH.100H₂O in aqueous solution modeled by COSMO show for the four conformations **3a** to **3d** absorption bands centered from 179 to 204 nm, corresponding to electronic transitions between orbitals located on the adenine moiety and orbitals located on the nicotinamide ring of NADPH. Moreover, due to the contribution of transitions from water molecules to orbitals located on NADPH, the intensity of these absorption maxima for NADPH.100H₂O is enhanced significantly comparing to NADPH. The maxima of the calculated bands corresponding to the experimental band at 260 nm are slightly blue shifted by 10 nm or less, whereas those related to the experimental band at 340 nm are red

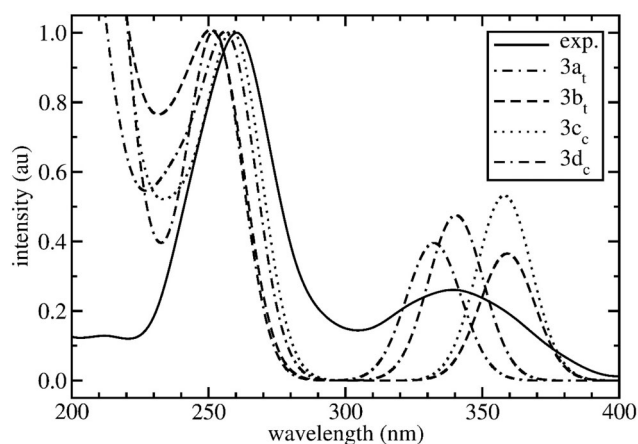


Figure 4. UV–vis absorption spectra of NADPH.100H₂O from TD-DFT/B3LYP calculations (basis sets A, $b = 0.005$, $\lambda > 200$ nm, COSMO for bulk water) in comparison to the experimental spectrum in aqueous solution^[10] (intensities in arbitrary units, AU). Only one representative of the *cis* and *trans* conformers of **3a–3d** is shown.

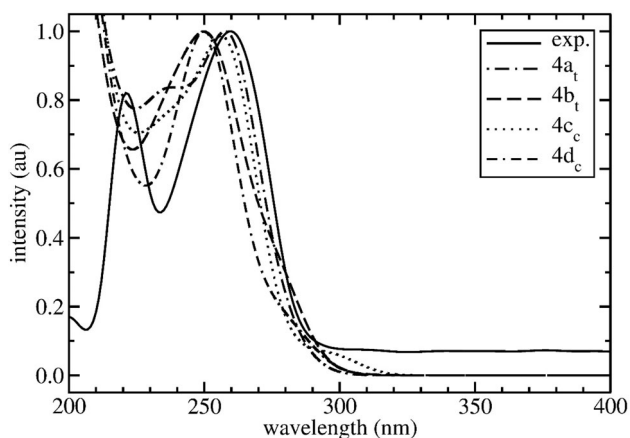


Figure 5. UV-vis absorption spectra of $\text{NADP}^+ \cdot 100\text{H}_2\text{O}$ from TD-DFT/B3LYP calculations (basis sets A, $b = 0.005$, $\lambda > 200$ nm, COSMO for bulk water) in comparison to the experimental spectrum in aqueous solution^[10] (intensities in arbitrary units, AU). Only one representative of the *cis* and *trans* conformers of **4a–4d** is shown.

shifted by at most 19 nm, compare Table 4. When setting the intensity maxima of the bands near 260 nm to 1.0, the intensities of the bands near 340 nm calculated in the length representation range between 0.36 and 0.53, that is, they are by up to a factor of two too large. In case of TDDFT/BP86 the agreement with the experimental spectrum is by far worse, for example, the calculated maxima of the bands corresponding to the experimental one at 340 nm are red shifted by 50–80 nm.

The TDDFT/B3LYP spectra for $\text{NADP}^+ \cdot 100\text{H}_2\text{O}$ in aqueous solution modeled by COSMO agree similarly well with the experimental spectrum as for the unoxidized form. The calculated maxima for the four energetically lowest conformations **4a** to **4d** corresponding to the experimental band at 259 nm are blue shifted by up to only 9 nm, compare Table 5. The calculated band maxima near 259 nm for NADP^+ (**4a–4c**) agree with those of NADPH (**3a–3c**) within 2 nm. The agreement is again worse for TDDFT/BP86, where besides a significant red shift of over 30 nm compared to the experimental band at 259 nm at least two additional bands between 300 and 450 nm are observed.

Table 4. Relative energies ΔE (kJ/mol) of low-energy conformers of NADPH in aqueous solution modeled by 100 explicitly treated water molecules and COSMO for bulk water from B3LYP calculations including zero-point energy corrections. Wavelengths of maxima (λ_{max} , nm) for the corresponding TDDFT/B3LYP UV-vis absorption spectra are also given (cf. Fig. 2 for structures **3a–3d**).

Structure	C	ΔE	λ_{max}
3a_c	7.96	31.5	347.1 (0.50), 256.9
3a_t	7.72	0.0	332.3 (0.39), 255.9
3b_c	6.21	27.8	344.4 (0.43), 250.3
3b_t	6.50	13.0	359.1 (0.36), 250.8
3c_c	6.28	29.4	358.1 (0.53), 258.4
3c_t	6.09	37.5	358.2 (0.49), 258.0
3d_c	6.25	138.4	340.4 (0.48), 250.8
Exp.			340, 260

Relative intensities unequal to 1.0 are listed in parentheses. Gaussian broadening parameter 0.005. C (Å) refers only to NADPH. Basis sets A.

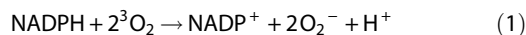
Table 5. Relative energies ΔE (kJ/mol) of low-energy conformers of NADP^+ in aqueous solution modeled by 100 explicitly treated water molecules and COSMO for bulk water from B3LYP calculations including zero-point energy corrections. Wavelengths of maxima (λ_{max} , nm) for the corresponding TDDFT/B3LYP UV-vis absorption spectra are also given (structures **4a–4d** are similar to **3a–3d**, cf. Fig. 2).

Structure	C	ΔE	λ_{max}
4a_c	7.74	12.3	257.7
4a_t	7.86	0.0	257.8
4b_c	6.18	8.5	251.4
4b_t	6.30	8.4	249.8
4c_c	6.18	11.8	256.1
4c_t	6.10	13.4	257.5
4d_c	6.53	99.8	256.6
Exp.			259

Gaussian broadening parameter 0.005. C (Å) refers only to NADP^+ . Basis sets A.

Oxidation of NADPH to NADP^+

Due to the high cost and pronounced instability of NADPH, intensive experimental work has been done to seek the best storage conditions.^[49] It was found that NADPH is labile in acids,^[7] and should be degassed (usually under N_2) prior to any measurement.^[48,50] Upon activation the NADPH oxidase of the cardiovascular system was found to catalyze the one electron reduction of oxygen in its triplet ground state, using NADPH as the electron donor^[51,52]:

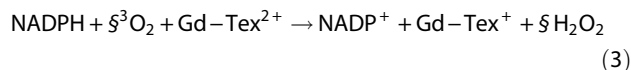


O_2^- together with H^+ can form HO_2 , from two of which H_2O_2 and O_2 can be obtained.

In the chemical system singlet oxygen reacts with NADPH to form NADP^{+53} :



Moreover, Magda et al. found that under aerobic conditions the cocubation of NADPH with Gd-TeX^{2+} converted the cofactor to its oxidized form.^[54] The hydrogen peroxide formation in a buffered solution of NADPH was determined by using a colorimetric method. They found that oxygen is serving as the ultimate electron acceptor under aerobic conditions. The corresponding oxidation of NADPH under aerobic conditions with Gd-TeX^{2+} may be written as:



The calculated changes of the Gibbs free energy ΔG in aqueous solution for the reactions (1)–(3), as well as reactions between NADPH and triplet oxygen, that is,



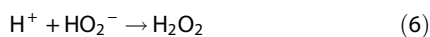
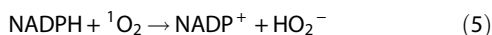
are listed in Table 6. For reaction (1) the obtained positive ΔG implies that the reaction could not proceed spontaneously, which agrees with the experimental observation, that is, the

Table 6. Calculated changes of Gibbs free energies ΔG (kJ/mol) in aqueous solution for the reactions: (a) $\text{NADPH} + 2 \text{}^3\text{O}_2 \rightarrow \text{NADP}^+ + 2 \text{O}_2^- + \text{H}^+$; (b) $\text{NADPH} + \text{}^1\text{O}_2 + \text{H}^+ \rightarrow \text{NADP}^+ + \text{H}_2\text{O}_2$; (c) $\text{NADPH} + \frac{1}{2} \text{}^3\text{O}_2 + \text{Gd-Tex}^{2+} \rightarrow \text{NADP}^+ + \text{Gd-Tex}^+ + \frac{1}{2} \text{H}_2\text{O}_2$; (d) $\text{NADPH} + \text{}^3\text{O}_2 + \text{H}^+ \rightarrow \text{NADP}^+ + \text{H}_2\text{O}_2$; (e) $\text{NADPH} + \text{}^1\text{O}_2 \rightarrow \text{NADP}^+ + \text{HO}_2^-$; (f) $\text{H}^+ + \text{HO}_2^- \rightarrow \text{H}_2\text{O}_2$.

ΔG	(a)	(b)	(c)	(d)	(e)	(f)
BP86	99	-298	-84	-143	-160	-138
B3LYP	93	-308	-95	-149	-171	-137

Basis sets B.

NADPH oxidase should be activated by intracellular second messengers or by upregulation of the component mRNAs.^[51] For reaction (2) and (3) the obtained negative ΔG values imply that the oxidation of NADPH by singlet oxygen or by Gd-Tex^{2+} are both exothermic, and therefore can proceed spontaneously. For the reaction of NADPH with triplet oxygen, that is, reaction (4), the obtained ΔG is also negative, implying the reaction (4) should proceed spontaneously too. However, a very slow reaction rate constant is expected, since the ground states of the reactants and products have different spin multiplicities, that is, $S = 3$ and $S = 1$ for $\text{NADPH} + \text{}^3\text{O}_2 + \text{H}^+$ and $\text{NADP}^+ + \text{H}_2\text{O}_2$, respectively. By taking the distance between H from NADPH and O from O_2 as the reaction coordinate, the scanned potential curve for the triplet state of $\text{NADPH} \cdot \cdot \text{O}_2$ is at least 88 kJ/mol energetically higher than the corresponding one for the singlet state of $\text{NADPH} \cdot \cdot \text{O}_2$, showing the nonexistence of STC (singlet-triplet crossing). For reaction (2) no reaction barrier was found, that is, with the decrease of the distance between H from NADPH and O from $\text{}^1\text{O}_2$, as well as the distance between H^+ and O from $\text{}^1\text{O}_2$, the energy of the system $\text{NADPH} \dots \text{}^1\text{O}_2 \dots \text{H}^+$ goes down to the product $\text{NADP}^+ + \text{H}_2\text{O}_2$. Moreover, the calculations showed that the reaction (2) can also proceed according to the following two steps:



or



The scanned potential curves for the reactions (5)–(8) showed that the reactants relax to the products with the decrease of the O–H distance, and no reaction barrier was found.

Conclusions

Energetically low-lying molecular structures of NADPH and its aromatic oxidized form NADP^+ were studied for the gas phase and the aqueous solution at the DFT level using the BP86 and B3LYP density functionals. Solvent effects were modeled with an explicit treatment of 100 water molecules in combination with the COSMO model for bulk hydration effects. It was found at the B3LYP level that the energetically lowest conformers of

NADPH/ NADP^+ exist in rather compact structures in gas phase due to the formation of various intramolecular hydrogen bonds between the terminal rings and the bridging unit. In aqueous solution most of these intramolecular hydrogen bonds are broken and replaced by intermolecular $\text{O} \cdot \cdot \text{H}$ hydrogen bonds to surrounding water molecules, resulting in more extended geometries than found for free NADPH/ NADP^+ in the gas phase. For both NADPH and NADP^+ the energetically lowest conformer in gas phase as well as in solution exhibits a *trans* orientation of the oxygen and the ring nitrogen atoms in the nicotinamide group. The UV–vis absorption spectra for NADPH and NADP^+ in aqueous solution calculated at the TDDFT/B3LYP level agree quite well with the experimental spectra, that is, the characteristic peak of NADPH at 340 nm appears to be red shifted by at most 19 nm, whereas the peaks at 260/259 nm of NADPH/ NADP^+ are blue shifted by at most 10 nm.


The changes of Gibbs free energies ΔG in reactions of NADPH with O_2 in the cardiovascular system and in the chemical system have been calculated and the obtained results agree with the experimental findings. For the oxidation reaction in the cardiovascular system, that is, $\text{NADPH} + 2 \text{}^3\text{O}_2 \rightarrow \text{NADP}^+ + 2 \text{O}_2^- + \text{H}^+$, the reaction cannot proceed without activation since the obtained ΔG is positive. The reaction of NADPH with singlet oxygen in the chemical system proceeds in two steps, that is, first the NADPH reacts with $\text{}^1\text{O}_2$ to form NADP^+ and HO_2^- , and then H_2O_2 is formed from H^+ and HO_2^- spontaneously.

Acknowledgment

The financial support of the Deutsche Forschungsgemeinschaft (DFG) CA 1390/1-1 is gratefully acknowledged.

Keywords: NADPH · density functional theory · molecular structure · electronic spectrum · oxidation reaction

How to cite this article: X. Cao, L. Wu, J. Zhang, M. Dolg. *J. Comput. Chem* **2020**, *41*, 305–316. DOI: 10.1002/jcc.26103

 Additional Supporting Information may be found in the online version of this article.

- [1] S. K. Spaans, R. A. Weusthuis, J. van der Oost, S. W. M. Kengen, *Front. Microbiol.* **2015**, *6*, 742.
- [2] W. J. Lennarz, D. M. Lane, Eds., *Encyclopedia of Biological Chemistry*, 2nd ed., Amsterdam: Academic Press, **2013**.
- [3] O. Carugo, P. Argos, *Proteins* **1997**, *28*, 10.
- [4] W. H. Ying, *Antioxid. Redox. Signal.* **2008**, *10*, 179.
- [5] Z. Y. Zhang, L. Chen, L. Liu, X. Y. Su, J. D. Rabinowitz, *J. Am. Chem. Soc.* **2017**, *139*, 14368.
- [6] D. H. Choi, J. Lee, *Int. J. Mol. Sci.* **2017**, *18*, 2500.
- [7] H. K. Chenault, G. M. Whitesides, *Appl. Biochem. Biotechnol.* **1987**, *14*, 147.
- [8] J. J. Tanner, S. C. Tu, L. J. Barbour, C. L. Barnes, K. L. Krause, *Protein Sci.* **1999**, *8*, 1725.
- [9] R. V. Hull, P. S. Conger, R. J. Hoobler, *Biophys. Chem.* **2001**, *90*, 9.
- [10] J. De Ruyck, M. Fameree, J. Wouters, E. A. Perpete, J. Preat, D. Jacquemin, *Chem. Phys. Lett.* **2007**, *450*, 119.

- [11] T. S. Blacker, R. J. Marsh, M. R. Duchon, A. J. Bain, *Chem. Phys.* **2013**, 422, 184.
- [12] O. S. Vasyutinskii, A. G. Smolin, C. Oswald, K. H. Gericke, *Opt. Spectrosc.* **2017**, 122, 602.
- [13] R. Ahlrichs, M. Bar, M. Haser, H. Horn, C. Kolmel, *Chem. Phys. Lett.* **1989**, 162, 165.
- [14] A. D. Becke, *Phys. Rev. A* **1988**, 38, 3098.
- [15] C. T. Lee, W. T. Yang, R. G. Parr, *Phys. Rev. B* **1988**, 37, 785.
- [16] A. D. Becke, *J. Chem. Phys.* **1993**, 98, 5648.
- [17] P. J. Stephens, F. J. Devlin, C. F. Chabalowski, M. J. Frisch, *J. Phys. Chem.* **1994**, 98, 11623.
- [18] C. Adamo, V. Barone, *J. Chem. Phys.* **1999**, 110, 6158.
- [19] M. Ernzerhof, G. E. Scuseria, *J. Chem. Phys.* **1999**, 110, 5029.
- [20] J. P. Perdew, *Phys. Rev. B* **1986**, 33, 8822.
- [21] A. Klamt, G. Schüürmann, *J. Chem. Soc. Perkin Trans.* **1993**, 2, 799.
- [22] Unpublished sets; TURBOMOLE basis set library. https://www.turbomole.org/wp-content/uploads/2019/10/Turbomole_Manual_7-4.pdf
- [23] A. Schafer, H. Horn, R. Ahlrichs, *J. Chem. Phys.* **1992**, 97, 2571.
- [24] F. Weigend, M. Haser, H. Patzelt, R. Ahlrichs, *Chem. Phys. Lett.* **1998**, 294, 143.
- [25] Y. Marcus, A. Loewenschuss, *J. Chem. Soc. Faraday Trans.* **1986**, 1, 2873.
- [26] L. Martinez, R. Andrade, E. G. Birgin, J. M. Martinez, *J. Comput. Chem.* **2009**, 30, 2157.
- [27] S. Grimme, C. Bannwarth, *J. Chem. Phys.* **2016**, 145, 054103.
- [28] T. A. Halgren, *J. Comput. Chem.* **1996**, 17, 490.
- [29] T. A. Halgren, *J. Comput. Chem.* **1999**, 20, 720.
- [30] N. M. O'Boyle, M. Banck, C. A. James, C. Morley, T. Vandermeersch, G. R. Hutchison, *J. Chem.* **2011**, 3, 33.
- [31] S. Grimme, J. Antony, S. Ehrlich, H. Krieg, *J. Chem. Phys.* **2010**, 132, 154104.
- [32] P. J. Knowles, H. J. Werner, *Chem. Phys. Lett.* **1985**, 115, 259.
- [33] P. J. Knowles, H. J. Werner, *Chem. Phys. Lett.* **1988**, 145, 514.
- [34] P. J. Knowles, H. J. Werner, *Theor. Chim. Acta* **1992**, 84, 95.
- [35] H. J. Werner, P. J. Knowles, *J. Chem. Phys.* **1988**, 89, 5803.
- [36] Human Metabolome Database 4.0. www.hmdb.ca (accessed 31st October 2019).
- [37] A. Moser, K. Range, D. M. York, *J. Phys. Chem. B* **2010**, 114, 13911.
- [38] E. P. L. Hunter, S. G. Lias, *J. Phys. Chem. Ref. Data Monogr.* **1998**, 27, 413.
- [39] C. Marian, D. Nolting, R. Weinkauff, *Phys. Chem. Chem. Phys.* **2005**, 7, 3306.
- [40] F. Turecek, X. H. Chen, *J. Am. Soc. Mass Spectrosc.* **2005**, 16, 1713.
- [41] G. De Luca, T. Marino, T. Mineva, N. Russo, M. Toscano, *J. Mol. Struct. Theochem* **2000**, 501, 215.
- [42] J. Zheng, Y. Q. Chen, R. Callender, *Eur. J. Biochem.* **1993**, 215, 9.
- [43] V. I. Polshakov, R. R. Biekofsky, B. Birdsall, J. Feeney, *J. Mol. Struct.* **2002**, 602, 257.
- [44] X. Cao, N. Heinz, J. Zhang, M. Dolg, *Phys. Chem. Chem. Phys.* **2017**, 19, 20160.
- [45] C. Latouche, D. Skouteris, F. Palazzetti, V. Barone, *J. Chem. Theory Comput.* **2015**, 11, 3281.
- [46] M. Caricato, G. W. Trucks, M. J. Frisch, K. B. Wiberg, *J. Chem. Theory Comput.* **2010**, 6, 370.
- [47] A. L. Lehninger, D. L. Nelson, M. Cox, Principles of Biochemistry, New York: Worth Publishers, **1993**.
- [48] E. J. Dell, F. Ganske, Detection of NADH and NADPH with the Omega's High Speed, Full UV/Vis Absorbance Spectrometer, Application Note170, BMG LABTECH, GmbH, Offenburg, Germany, **2008**.
- [49] J. T. Wu, L. H. Wu, J. A. Knight, *Clin. Chem.* **1986**, 32, 314.
- [50] J. Chen, C. X. Cai, *Chin. J. Chem.* **2004**, 22, 167.
- [51] K. K. Griendling, D. Sorescu, M. Ushio-Fukai, *Circ. Res.* **2000**, 86, 494.
- [52] B. M. Babior, *Blood* **1999**, 93, 1464.
- [53] R. S. Bodaness, P. C. Chan, *J. Biol. Chem.* **1977**, 252, 8554.
- [54] D. Magda, C. Lepp, N. Gerasimchuk, I. Lee, J. L. Sessler, A. Lin, J. E. Biaglow, R. A. Miller, *Int. J. Radiat. Oncol.* **2001**, 51, 1025.

Received: 10 July 2019

Revised: 3 October 2019

Accepted: 16 October 2019

Published online on 11 November 2019